Journal of The Electrochemical Society, **153** (1) C33-C36 (2006)
0013-4651/2005/153(1)/C33/4/$15.00 © The Electrochemical Society, Inc.

Preparation of Ultramicroelectrode Array of Gold Hemispheres on Nanostructured NiAl–Re

Belen Bello Rodriguez, André Schneider, and Achim Walter Hassel*,z

Max-Planck-Institut für Eisenforschung GmbH, 40237 Düsseldorf, Germany

Nanopore arrays prepared by partial dissolution of the fibrous phase present in a directionally solidified NiAl–Re eutectic alloy were employed as starting material for the design of arrays of microelectrodes. Polycrystalline gold hemispheres have been grown onto the created nanopores by electrodeposition. The applied pulses resulted in the formation of gold nuclei that grew to fill up the pores. After complete cover of the pores, the application of further pulses resulted in the deposition of more gold particles onto the existing ones, creating microspheres with a diameter of 2–4 μm and evenly distributed on the rhenium pores. Polarization of the sample prior to the gold electrodeposition ensured formation of passive oxides on the matrix of the NiAl–Re samples, thus favoring the selective plating of gold onto the pores only. The resulting arrays of gold microspheres showed a good electrochemical performance when voltammetric analysis of Fe(II)/Fe(III) was carried out, which demonstrates the suitability of the deposits as electrochemical microsensors. A subsequent selective dissolution of the matrix revealed a structure which is in full agreement with the proposed model. Gold hemispheres (2–4 μm diam) reside on top of rhenium nanowires (400 nm diam). These spheres showed a sufficient mechanical stability and adherence to the parallel aligned nanowires.
 [DOI: 10.1149/1.2130567]

Manuscript submitted July 22, 2005; revised manuscript received September 2, 2005. Available electronically November 29, 2005.

Creation of micro and nanoelectrodes is of continuous interest due to the improved performance that such devices can show when compared to conventional electrodes. The fabrication of arrays of geometrically identical and well-defined nano- or microstructures opens their applicability as sensors for electroanalytical purposes.[1] Arrays of micro- or nanoelectrodes are specially applied in the fields of biotechnology or immunosensing, because the size of the sensors can match that of the measured compounds.[2-4] Arrays of microelectrodes have also proved useful as environmental sensors, where their improved sensitivity is a bonus for the detection of concentrations below the detection limit of conventional methods.[5] Formation of small-size electrodes with high aspect ratios has been traditionally carried out by electrodeposition on etched ion tracks in foils or templates.[6] From the possible metals to deposit, gold has attracted much interest due to its application in catalysis, in DNA sequence determination, microscopy, and electronics.[7,8] The production of arrays of microstructures on substrates by lithographic techniques presents the disadvantage of high cost and a restriction in the number of materials to which it can be applied. The method can also prove complex and inefficient. Template-based methods overcome those disadvantages, but the obtained structures often present a high number of imperfections due to packing defects in the original templates.[9] We have recently reported on the production of arrays of nanopores and nanowires from directionally solidified eutectics.[10,11] The use of eutectics has the advantage of allowing the production of self-organized nanostructures of large aspect ratios. By conveniently controlling the conditions of the eutectic growth, a final microstructure can be obtained with nanofibers parallel to the growth direction.[12] The method is extensible to any system that shows eutectic properties but can also be exploited for the formation of arrays of nano- or microstructures by electrodeposition of the appropriate metal onto the created fibers. For our studies, we chose a pseudobinary NiAl–Re eutectic which can easily be polarized in neutral acetate buffer for the formation of nanopore arrays.[10] By carefully controlling the potential and maintaining a neutral pH, the formation of nanopores occurs simultaneously with the passivation of the NiAl matrix due to the formation of Al_2O_3.[13] The selective electrodeposition of gold onto the obtained nanopores yields the formation of arrays of gold microspheres adjacent to each other. The obtained gold bumps showed a good electrochemical performance after initial investigation with the benchmark redox system Fe(II)/Fe(III). This good electrochemical response shows the potential of the created structures as arrays of microelectrodes.

* Electrochemical Society Active Member.
z E-mail: hassel@elchem.de

Materials and Methods

NiAl–Re eutectics were solidified according to a procedure previously developed.[10] As a starting material, nickel (99.97 wt %), electrolytic aluminum (99.9999 wt %), and rhenium pellets (99.9 wt %) were used for the alloy preparation. The directional solidification was conducted at a temperature of 1690 ± 10°C, a thermal gradient of approximately 40 K/cm, and a growth rate of 8.3 μm/s. The microstructure of the obtained unidirectionally solidified NiAl–Re 1.25 eutectic was examined by scanning electron microscopy (SEM) and energy-dispersive X-ray (EDX) analyses and exhibited a fully eutectic morphology consisting of a cell structure with a mean cell diameter of 1.5 mm. The mean diameter of the Re fibers in the eutectic cells was about 400 nm, while the mean interfiber spacing was 3 μm. The fiber orientation was ⟨1120⟩, referring to the rod axis of the directionally solidified sample.[10]

The partial dissolution of the rhenium fibers was accomplished electrochemically by polarization of the eutectic alloy in 1 M acetate buffer (pH 6.0) at 0.702 V [vs saturated hydrogen reference electrode (SHE)] for 3 min at room temperature and after deaeration. A conventional three-compartment cell (approximately volume 50 mL) with working, reference, and auxiliary electrodes was employed in all experiments. The fabricated NiAl–Re alloy was cut in 1-mm-thick plates (apparent surface area 1 cm^2) and mechanically ground and mirror-like polished prior to measurements. A commercial Ag/AgCl electrode was used as reference (Metrohm, Filderstadt, Germany). A smooth Au foil electrode was employed as counter (apparent surface area 2 cm^2). A PST050 potentiostat (Radiometer Analytical, Lyon, France) was used in all electrochemical measurements. Measurements were performed at room temperature in deaerated and quiescent solutions. The obtained pores had a depth of approximately 280 nm.

Electrodeposition of gold was carried from a commercial bath containing 12 g L^{-1} of gold sulfite in neutral pH (Metakem, Usingen, Germany). After pores formation, the NiAl–Re samples were placed in the electrochemical cell alongside the Au foil which acted as anode during the electrodeposition. The plating was carried out by application of rectangular reverse pulses[14] from a PST050 potentiostat, as schematized in Fig. 1. The potential was switched from −0.7 to 0.1 V (against anode) at a ratio of 3:1 s. All experiments were performed at room temperature in nondeaerated solutions.

For the characterization of the produced gold microstructures, cyclic voltammograms were performed in the presence of 0.1 and 0.01 M ferrocyanide solutions. A three-electrode configuration cell was also employed for these tests, consisting of a commercial Ag/AgCl reference electrode and a gold foil counter electrode.

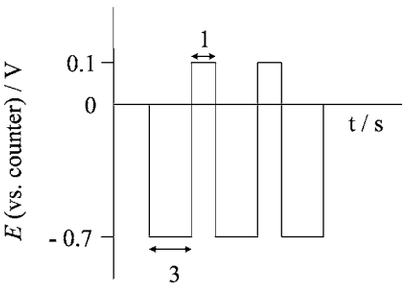

Figure 1. Schematic representation of the reverse polarization pulses applied for gold electrodeposition.

NiAl–Re samples onto which gold was deposited were employed as working electrodes. The voltammograms were recorded after deaeration of the solution in quiescent conditions.

The partial dissolution of the NiAl matrix after deposition of gold spheres was performed as a quick and alternative investigation on the exclusive deposition of gold on rhenium fibers. The NiAl matrix was partially etched, according to a procedure previously described,[11] by digestion of the samples in solutions containing 3% H_2O_2 and 3.2% HCl.

SEM pictures were obtained on a Leo 1550 VP apparatus (Leo Elektronenmikroskopie GmbH, Oberkochen, Germany) fitted with an INCA energy dispersive system (EDS) (Oxford Instruments, Oxford, U.K.).

All materials used were of analytical grade and purchased from Merck (Darmstadt, Germany).

Results and Discussion

Deposition of gold structures onto rhenium nanofibers.— The passivation of the NiAl–Re alloy, along with the dissolution of the Re phase, has been discussed earlier and is beyond the scope of the current manuscript.[10] A polarization in neutral acetate buffer was carried out to favor the formation of Ni(II) and Al(III) oxides and the simultaneous dissolution of Re as perrhenate. Only a short treatment was performed, enough to create pores with an approximate depth of 200–300 nm, to avoid limitations in the diffusion of the gold ions into the pore surfaces. Polarization of the samples proved essential for a selective deposition of gold, because the formation of both NiO and Al_2O_3 oxides ensures that only the rhenium fibers remain electrochemically active. The partial dissolution of rhenium and the subsequent formation of pores also favors the creation of gold deposits strictly organized as arrays onto the fibrous phase. The electrodeposition of gold was carried out by alternating the applied current from cathodic to anodic values. Analysis of the data recorded during the process showed an initial increase in the cathodic current to an approximate value of 84 $\mu A\ cm^{-2}$, which became stable after a short deposition period (8 s). For polarization times between 8 and 18 s, the current increased slowly to 103 $\mu A\ cm^{-2}$. The increase in current became more dramatic for longer times and followed a linear relationship in the range 19–250 s. For times >250 s, the increase in current density was smoother and seemed to reach a steady state at 1.2 mA after deposition for 500 s (Fig. 2a). The integrated charge displayed in Fig. 2b also became more negative with longer deposition times, following a sigmoidal curve throughout the studied range (0–600 s). The initial low current recorded after short deposition times (<8 s) could be due to the pore filling. The slow increase in the current value observed after this initial stage may be triggered by the initiation of the growth of gold deposits onto the filled pores (8–18 s). The subsequent increase observed for the recorded current (for deposition times >19 s) would therefore be due to the growth of gold particles onto the initially formed gold nanowires within the pores. The final stabilization of the current value suggests that the growth of gold deposits is controlled by the diffusion of ions after deposition times >250 s. This interpretation is coherent with proposed mechanisms for the formation of gold deposits on tracks.[15] The calculated mass of gold deposited also increased more rapidly for deposition times in the range 0–600 s. From then on, the gold mass did not change dramatically.

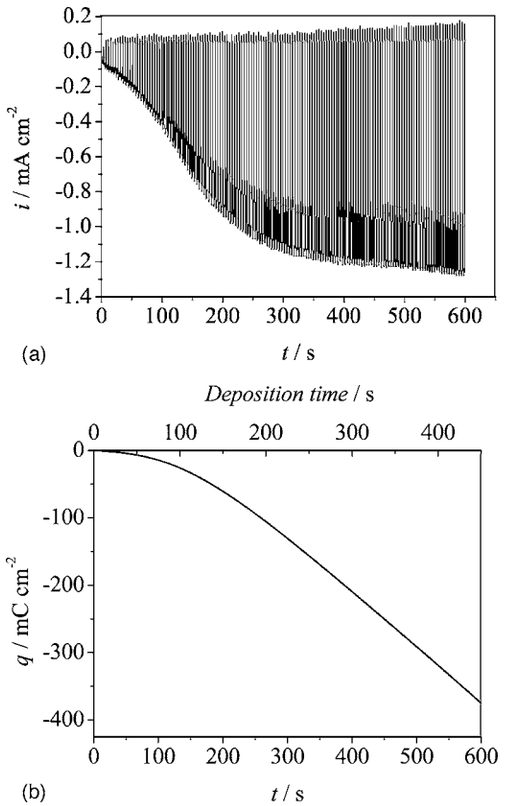

Figure 2. (a) Current density recorded over polarization time for the application of cathodic and anodic pulses (ratio 3:1 s) on a passivated NiAl–NRe eutectic (working electrode). A gold foil was employed as counter electrode. (b) Charge obtained after integration of the recorded i vs t plot (same conditions as expressed for Fig. 2a).

The whole process could be interpretated as a progressive nucleation followed by a diffusion-controlled growth.[16] Each of the pulses applied for the electrodeposition creates a gold nucleus in the electrochemically active pore. New nuclei grow with further treatment until complete filling of the pores. Once the surface of the pore is completely covered by gold, the subsequent pulses applied results in the formation of further gold nuclei that now grow on the existing gold deposits. The final structure comprises of spheres held on rhenium nanofibers. Without the initial formation of pores, the growth of gold deposits onto each other would occur much earlier. The resulting deposits would therefore be larger than those observed when an initial pore filling took place. Overlapping among consecutive deposits would be more likely, thus reducing the possibilities of any creation of arrays of microelectrodes. This effect was observed when unpassivated samples were exposed to the electrodeposition procedure.

SEM images of the deposited gold structures (Fig. 3) showed small particles of 1–2 μm size onto the rhenium pores for deposition times <180 s. Those particles seem to be formed by smaller spheres that grew together. The application of series of pulses may originate single gold particles after each pulse that will deposit on the electrochemically active pore. The application of a small number of pulses results in the formation of only a few particles, perfectly discriminated from each other. Longer deposition periods resulted in the formation of more defined spheres with diameters in the 4–6

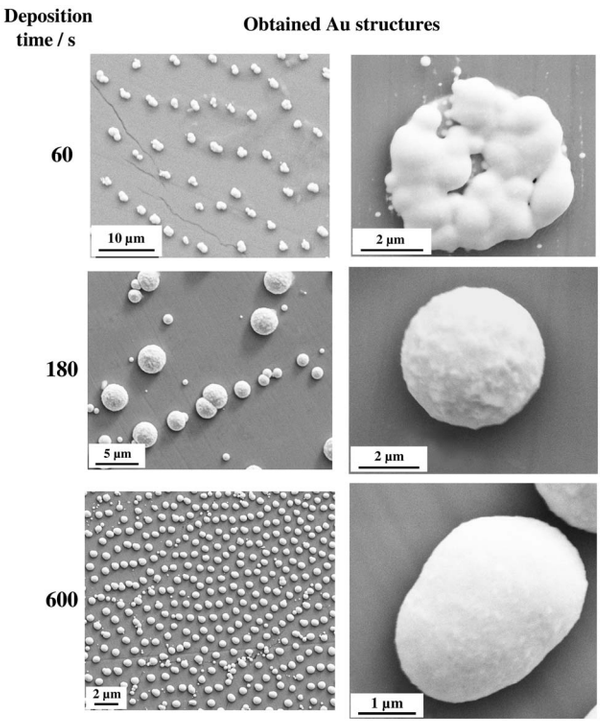

Figure 3. SEM images of gold deposits obtained on passive NiAl–Re samples after different polarization times.

-µm range (for deposition times 180–600 s). These spheres are understood to be formed by the overlapping of gold particles originated after the application of consecutive pulses. After the initial filling of the pore, deposition proceeds on the gold particles, thus resulting in a better defined morphology of the final structures.

Chemical digestion of samples after gold deposition.— Deposition of gold took place exclusively in the pores left by the partial dissolution of the rhenium fibers. This was demonstrated with the chemical digestion of the NiAl matrix in a mildly oxidant solution. The 3% H_2O_2 and 3.2% HCl mixture employed for this procedure allowed the selective dissolution of the less noble of the components, thus leaving intact the rhenium and gold structures. SEM images obtained after dissolution of the matrix displayed

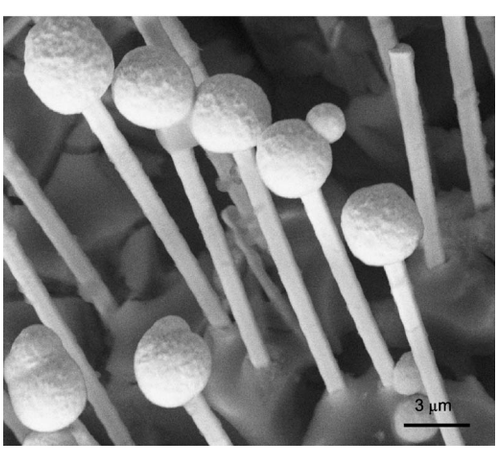

Figure 4. SEM image of gold microspheres deposited onto rhenium nanofibers after chemical etching of the NiAl matrix.

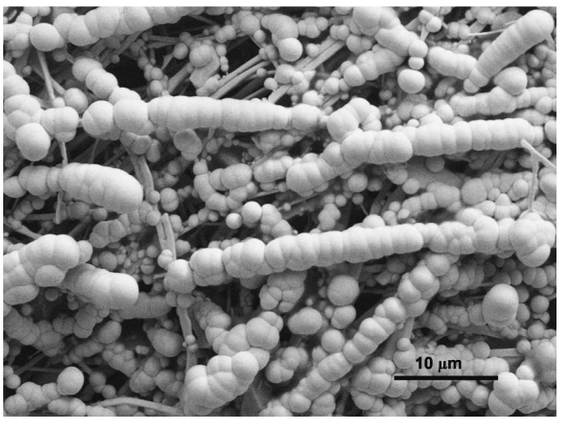

Figure 5. SEM image of gold deposits obtained when the NiAl–Re samples are not preconditioned for passivation of the NiAl matrix.

mushroom-type hemispheres onto the rhenium nanowires. X-ray scans performed on the visualized structures showed a profile for gold concentration that decreased when moving along the fiber. No gold was found on other sections of the samples, demonstrating the suitability of the initial passivation procedure for the creation of electrochemically active pores (Fig. 4).

Electrodeposition of gold on non-passivated samples.— It was observed that plating of gold on samples that had not been previously exposed to the passivation conditions displayed many inhomogeneous gold deposits distributed on the whole of the sample surface (Fig. 5). In this case it can be concluded that the obviation of the pretreatment favors the presence of electrochemically active centers outside the rhenium fibers. The subsequent application of a cathodic potential produces nucleation centers distributed throughout the entire surface of the sample. The absence of a pore-filling step in the process also produces larger deposits, because the growth of spheres starts as soon as the nucleation centers are created. The formation of arrays of gold microelectrodes was therefore hindered by the overall distribution of the plating metal.

Electrochemical characterization of arrays of gold microspheres.— The electrodeposition procedure described in the current manuscript allows the formation of arrays of gold microelectrode onto a stable and robust template (passive NiAl). Preliminary investigations on the electrochemical performance of the obtained

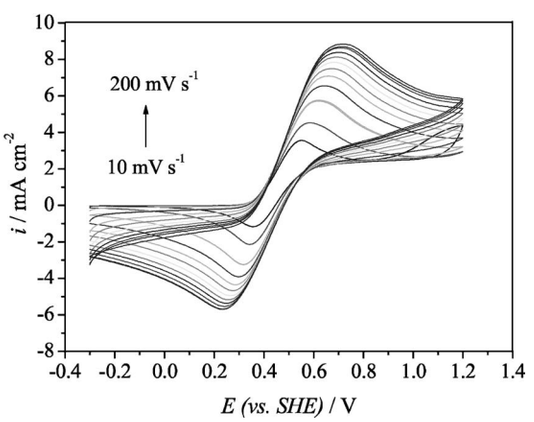

Figure 6. Cyclic voltammograms recorded for 0.1 M ferrocyanide at different scan rates. The gold microspheres deposited onto the rhenium fibers (after 5 min polarization) were employed as working electrode. An Ag/AgCl electrode was used as reference and a gold foil as counter electrode.

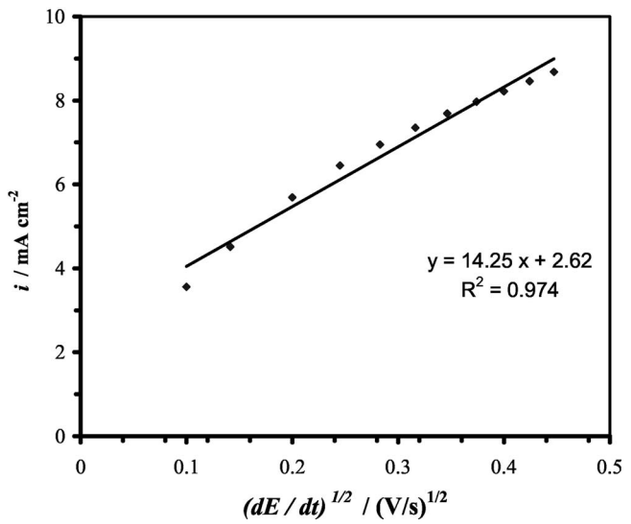

Figure 7. Increase in the anodic peak current with scan rate for 0.1 M ferrocyanide as recorded with the array of deposited gold structures as working electrode. A commercial Ag/AgCl electrode was employed as reference, and a gold foil as counter electrode.

arrays were carried out in the presence of the benchmark redox couple Fe(II)/Fe(III). Cyclic voltammograms recorded for solutions containing 0.1 M and 0.01 M Fe(II) displayed well-defined oxidation and reduction peaks (Fig. 6). Both peaks were slightly shifted with increasing scan rates, resulting in a larger peak separation for larger scan rates (200–300 mV). This separation is much greater than the theoretical peak separation of 58 mV for a reversible one-electron-transfer reaction, suggesting that the reaction taking place on the gold microelectrodes is not completely reversible. Overall, the anodic peak was observed in the 0.4–0.8 V range, with the cathodic peak appearing in the 0.4–0.2 V range (vs SHE). The peak height also increased linearly with the square root of the scan rate (Fig. 7). The electrode active area calculated from this linear relation (considering the Randles equation) was 21% of the geometric area [for 0.1 M Fe(II)]. The presence of well-defined peaks, instead of limiting currents, suggests a planar diffusion layer rather than a spherical one.

Conclusion

Gold microstructures with a diameter of 2–3 μm have been successfully electrodeposited into pores previously created on the surface of directionally solidified NiAl–Re eutectic alloys. A preliminary polarization of the alloy in a neutral medium ensures the passivation of the NiAl matrix and the partial dissolution of the rhenium fibers to form nanopores. The subsequent reversal of the electrodeposition current allows the exclusive deposition of gold into the pores. The electrodeposition process is thought to be determined by the initial formation of nucleation centers inside each of the pores, followed by the growth of the nuclei until complete filling of the pores. The application of further reverse pulses results in the growth of gold deposits onto the already plated pores. The exclusive deposition of gold spheres onto the pores favored the formation of arrays of gold microelectrodes. Preliminary investigations on the electrochemical behavior of such arrays suggested their suitability for use as electrochemical sensors.

Acknowledgments

Financial support of the Deutsche-Forschungs-Gemeinschaft through the project Production of Nanowire Arrays through Directional Solidification and their Application within the DFG Priority Program 1165 Nanowires and Nanotubes-from Controlled Synthesis to Function is gratefully acknowledged. The authors are also grateful to Dr. Srdjan Milenkovic for solidification of the employed eutectics.

Max-Planck-Institut fur Eisenforschung GmbH assisted in meeting the publication costs of this article.

References

1. H. J. Lee, C. Beriet, R. Ferrigno, and H. H. Girault, *J. Electroanal. Chem.*, **502**, 138 (2001).
2. P. Van Gerwen, W. Laureyn, W. Laureys, G. Huyberechts, M. Op De Beeck, K. Baert, J. Suls, W. Sansen, P. Jacobs, L. Hermans, and R. Mertens, *Sens. Actuators B*, **49**, 73 (1998).
3. S. M. Radke and E. C. Alocilja, *Biosens. Bioelectron.*, **20**, 1662 (2005).
4. K. Dill, D. D. Montgomery, A. L. Ghindilis, K. R. Schwarzkopf, S. R. Ragsdale, and A. V. Oleinikov, *Biosens. Bioelectron.*, **20**, 736 (2004).
5. J. Pritchard, K. Law, A. Vakurov, P. Millner, and S. P. J. Higson, *Biosens. Bioelectron.*, **20**, 765 (2004).
6. D. Dobrev, J. Vetter, and N. Angert, *Nucl. Instrum. Methods Phys. Res. B*, **149**, 207 (1999).
7. P. R. Selvakannan, S. Mandal, R. Pasricha, and M. Sastry, *J. Colloid Interface Sci.*, **279**, 124 (2004).
8. E. Sibert, F. Ozanam, F. Maroun, R. J. Behm, and O. M. Magnussen, *Surf. Sci.*, **572**, 115 (2004).
9. M. A. Ghanem, P. N. Bartlett, P. de Groot, and A. Zhokov, *Electrochem. Commun.*, **6**, 447 (2004).
10. A. W. Hassel, B. Bello Rodriguez, S. Milenkovic, and A. Schneider, *Electrochim. Acta*, **50**, 3033 (2005).
11. A. W. Hassel, B. Bello Rodriguez, S. Milenkovic, and A. Schneider, *Electrochim. Acta*, **51**, 795 (2005).
12. K. A. Jackson and J. D. Hunt, *Trans. Metall. Soc. AIME*, **236**, 1129 (1966).
13. M. Pourbaix, *Atlas of Electrochemical Equilibria in Aqueous Solutions*, pp. 300–306, National Association of Corrosion Engineers, Houston, TX (1974).
14. D. Dobrev, J. Vetter, N. Angert, and R. Neumann, *Electrochim. Acta*, **45**, 3117 (2000).
15. W. Kautek, S. Reetz, and S. Pentzien, *Electrochim. Acta*, **40**, 1461 (1995).
16. L. M. Depestel and K. Strubbe, *J. Electroanal. Chem.*, **572**, 195 (2004).